Journal of the Korean Society of Surveying, Geodesy, Photogrammetry and Cartography
Vol. 33, No. 3, 203-209, 2015
http://dx.doi.org/10.7848/ksgpc.2015.33.3.203

ISSN 1598-4850(Print)
ISSN 2288-260X(Online)
Original article

Effectiveness of Using the TIR Band in Landsat 8 Image Classification

Lee, Mi Hee[1] · Lee, Soo Bong[2] · Kim, Yongmin[3] · Sa, Jiwon[4] · Eo, Yang Dam[5]

Abstract

This paper discusses the effectiveness of using Landsat 8 TIR (Thermal Infrared) band images to improve the accuracy of landuse/landcover classification of urban areas. According to classification results for the study area using diverse band combinations, the classification accuracy using an image fusion process in which the TIR band is added to the visible and near infrared band was improved by 4.0%, compared to that using a band combination that does not consider the TIR band. For urban area landuse/landcover classification in particular, the producer's accuracy and user's accuracy values were improved by 10.2% and 3.8%, respectively. When MLC (Maximum Likelihood Classification), which is commonly applied to remote sensing images, was used, the TIR band images helped obtain a higher discriminant analysis in landuse/landcover classification.

Keywords : Landsat 8, TIR Image, Band Combination, Visible and Near Infrared Image, Maximum Likelihood Classification

1. Introduction

Due to rapid urbanization, various environmental problems such as urban heat island effects, water pollution, and atmospheric pollution have emerged. Because of a rising demand for environment-related information, it has become more important to acquire environmental data from diverse sources and distribute them. The data from a local area are not sufficient to assess and predict environmental changes. In other words, accurate data may not be acquired unless both intensive and extensive sources are available. Therefore, it is necessary to unite environmental data from extensive areas such as satellite images with environmental sensor data from small intensive areas (Lee *et al*., 2014; Park *et al*., 2014). The extensive sources from which environmental data are extracted are usually obtained through satellite images. Among observation satellite images, Landsat has been in operation since 1972. For decades, huge amounts of Landsat images have been accumulated and studied (Erdenechimeg *et al*., 2010; Jensen, 2007). From the Landsat TIR band, surface temperatures can be extracted. In addition, there have been many studies on the extraction of more accurate temperature data (Schneider and Mauser, 1996; Zhang *et al*., 2006). Processed results from the TIR band can be used for various applications such as ecological park management, management of parks and green areas, and geothermal area searches fused with diverse image technologies (Moon *et al*., 2012). Thus far, the TIR band has not been widely used

Received 2015. 05. 26, Revised 2015. 06. 08, Accepted 2015. 06. 24
1) Member, Dept. of Advanced Technology Fusion, Konkuk University (E-mail: mihee7586@konkuk.ac.kr)
2) Member, Dept. of Advanced Technology Fusion, Konkuk University (E-mail: wimi8484@konkuk.ac.kr)
3) Senior Research Associate, National Disaster Management Institute, Seoul 121-719, Korea (E-mail: lovefortajo@gmail.com)
4) Division of Interdisciplinary Studies, Dept. of Advanced Technology Fusion, Konkuk University (E-mail: lifelove@konkuk.ac.kr)
5) Corresponding Author, Member, Division of Interdisciplinary Studies, Dept. of Advanced Technology Fusion, Konkuk University (E-mail: eoandrew@konkuk.ac.kr)

in image classification aimed to extract an actual urban area because its spatial resolution is lower than that of other visible and near-infrared bands. However, there have been studies on the improvement of classification accuracy with the TIR band's temperature information (Warner and Nerry, 2009). In addition, TIR images that provide land surface temperature information, despite low spatial resolution, can be used as a substitute for visible and near-infrared images (Jung and Park, 2014). Some studies have been steadily progressing to enhance the spatial resolution of TIR images (Jeganathan *et al*., 2011; Jung and Park, 2014). This study investigated the effects of TIR band images on the improvement of classification accuracy at the landuse/landcover classifications using Landsat 8 satellite images and reviewed the results.

2. Data and Preprocessing

2.1 Study area and image data

An area that includes Seoul, the capital of the Republic of Korea, was selected as the study area. To figure out the accuracy of classification images, land cover in the target area should be evenly distributed. In this study, an urban region, crop, watershed, and forest are evenly distributed in a target area. The study area is shown in Fig. 1.

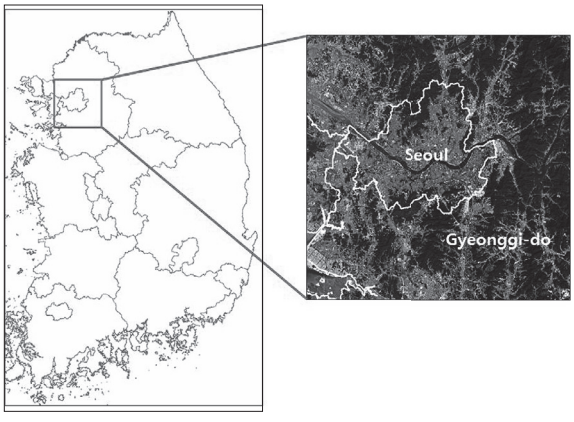

Fig. 1. Study area

The satellite image used in the experiment is from Landsat 8 (WRS-2, Path: 116, Row: 34) and was acquired on October 5, 2014. The level of image correction is the level-1T corrected provided from the USGS (United States Geological Survey). This was captured in early autumn, and a status of tree distribution can be seen with the naked eye.

The Landsat 8 satellite acquires images using two sensors, nine shortwave bands in the OLI (Operational Land Imager), and the TIR sensor's two long wave bands. In this study, seven multi-bands were used except for Band 1, which was designed to discover a coastal area and particles such as dust, and Band 9, which was targeted to find clouds. Fig. 2 reveals the overall flow of the experiment.

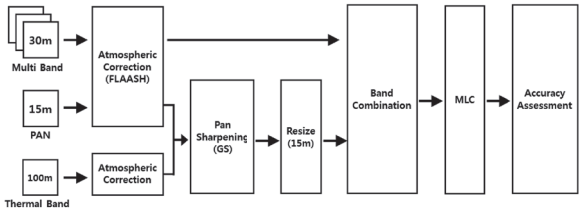

Fig. 2. Experiment flow

2.2 Atmospheric correction

A satellite sensor generates images by detecting energy radiated from the surface. This energy is further scattered and absorbed by the atmosphere before reaching the sensor (Lee *et al*., 2015). For this reason, atmospheric correction was carried out. ENVI's (Environment for Visualizing Images) FLAASH (Fast Line-of-sight Atmospheric Analysis of Spectral Hypercubes) module was used for correction of visible and near-infrared bands because FLAASH offered the wavelength from the visible to mid-infrared bands. In the FLAASH module, we can choose the atmospheric model in MODTRAN (MODerate resolution atmospheric TRANsmission) (FLAASH, 2009).

Table 1. FLAASH input parameters

Image Center Location	37°31′22.03″N 127°02′02.22″E
Sensor Altitude	705km
Ground Elevation	0.2km
Pixel Size	30m
Flight Date	Oct. 5, 2014
Flight Time GMT	02:11;14
Atmospheric Model	Sub-Arctic Summer (SAS)
Initial Visibility	20km

The input values in the FLAASH module are stated in Table 1. Among the input values, SAS (Sub-Arctic Summer) which meets weather and atmospheric conditions at the time of image acquisition-was chosen as the atmospheric model.

Because the FLAASH module does not support atmospheric correction in TIR band images, Eq. (2), proposed by Coll *et al.* (2010), was additionally used for TIR images. In terms of atmospheric correction in TIR band images, the DN (Digital Number) is converted into radiance. For this conversion, Eq. (1) was adopted (Chander and Markham, 2003). The gain and offset used in Eq. (1) were acquired from the images' metadata. Using Eq. (2), in addition, atmospheric correction was done.

$$Rad = gain \cdot DN + offset \quad (1)$$

$$Rad_{ac} = \frac{Rad - L_U}{\varepsilon \cdot \tau} - \frac{1-\varepsilon}{\varepsilon} L_D \quad (2)$$

where, Rad_{ac}: the atmospherically corrected cell value as radiance, Rad: the cell value as radiance, L_U: upwelling radiance, L_D: downwelling radiance, τ: transmittance, and ε: emissivity.

Each variable was obtained from the website (http://atmcorr.gsfc.nasa.gov/) provided by the NASA (National Aeronautics and Space Administration). Because Band 11 is unable to estimate the amount of distributed light from a sensor, only Band 10 is now provided; therefore, for a Landsat 8 TIR band, Band 10 was chosen in this study.

2.3 TIR image sharpening

To use TIR image at land classification, TIR image sharpening was conducted. That is, the TIR band images with low spatial resolution were spatially sharpened with PAN (PANchromatic) images with high spatial resolution. The TIR image sharpening method was motivated from image fusion. The image fusion method is a technique aimed to make multi-spectral images with improved spatial resolution by mathematically uniting the PAN images with high spatial resolution with multi-spectral images with high spectral resolution (Lee *et al*., 2014). This image fusion method can be divided into the MRA (Multi-Resolution Analysis) based method and CS (Component-Substitution) based method (Choi, 2011; Kim, 2008). In the CS based fusion method, differences between low resolution virtual satellite images artificially created using multi-band images and PAN images are applied to multi-band images. In this study, the GS (Gram-Schmidt) fusion technique, which preserves the image's DN in an effective manner and is the best in terms of performance, was used among the CS-based algorithms (Choi and Kim, 2010). For this, ENVI software was adopted. To have the TIR sharpened image match with the OLI's image bands, resampling was conducted in 30m resolution. The nearest neighborhood interpolation method, a typical image resampling technique in remote sensing image processing, was used. The TIR sharpened image is shown in Fig. 3.

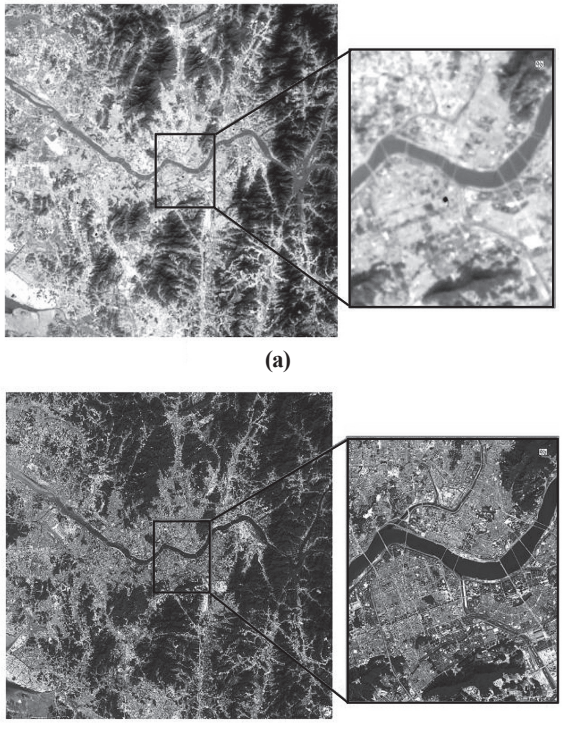

(a)

(b)

Fig. 3. TIR sharpened image, (a): original TIR image, (b): TIR sharpened of PAN and TIR images

3. Experiment and Analysis

To secure the generality of the study results, this study used MLC, which is often available as a remote sensing

image classifier. The MLC is one of the most common methods designed to classify satellite images using remote sensing, which is dependent upon the distribution and probability of training data (Sugumaran *et al*., 2003). The class is selected based on the landcover/landuse classification system of the USGS. If the spatial resolution of Landsat images is considered, it belongs to Level 1. Therefore, a total of seven classes (forest, water, field, paddy field, grass, dry stream, and urban area) included in Level 1 were chosen (Eo, 1999). Due to the limitations of the images' spatial and spectral resolution, field and paddy field were classified as crop. The number of pixels used in the training area are listed Table 2.

Table 2. Number of pixels used in the training area

Training area	Forest	Water	Crop	Grass	Dry stream	Urban
The number of pixels	5225	1359	969	450	240	2000

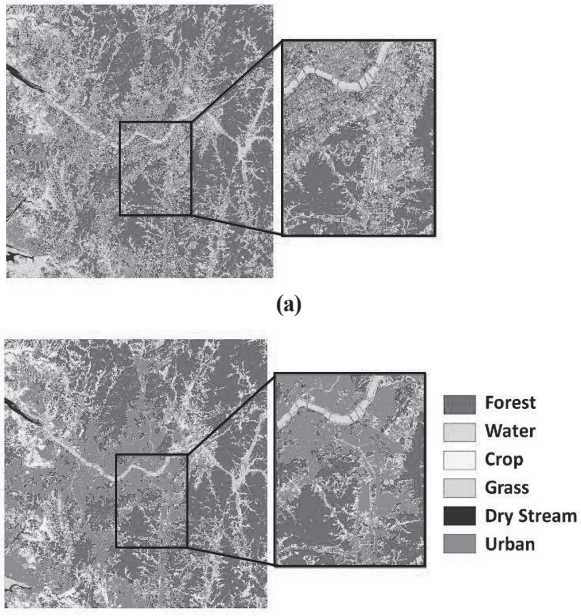

(a)

(b)

Fig. 4. Land cover classification by MLC, (a): classification image only using the multispectral image, (b): classification image using the multispectral image with TIR band added

Fig. 4 shows the classification result obtained by using MLC. The urban and crop regions can be seen to have been better classified.

According to the results of the land cover classification of the band combined to determine band combination based on the study written by Kwon *et al*. (2003), high accuracy was found in a combination of three or four bands among the band combinations classified within the top 10 in terms of accuracy (Eo, 1999; Kwon *et al*., 2003). In general, even though all six bands-except the TIR band-are used in Landsat image classification, the accuracy of the results is still low in ranking. Therefore, it is not always true that the use of many bands during satellite-based land cover classification will enhance the accuracy of classification. Among band combinations classified within the top 10, in this study, those combined with three or four bands were selected and experimented on with the addition of a TIR band (Kwon *et al*., 2003).

For accuracy assessment, in this study, 100–300 reference points were set for each class through systematic sampling for the collection of ground truth data. For the classes with a lack of reference points, random sampling was added.

In addition, a TIR band was added to the combination of the multi-bands that were selected to examine accuracy improvement. Lastly, each multi-band was substituted with a TIR band after extracting the number of cases in three combination bands in terms of the multi-band combinations in Table 3 for the purpose of discovering a band whose accuracy decreases when a TIR band is added to the multi-band combination. According to the experiment, the highest overall accuracy at classification of only multi-images was overall accuracy 83.2% in the 3, 5 and 7 band combinations in Case #5. When classified by including a TIR band in the multi-images of Case #5, an overall accuracy of 84% was observed, which was the highest among the TIR band–included combinations.

When classified including TIR bands, the band combinations with the most improved accuracy were TIR, 5 and 7 in Case #8. Among the overall band combinations, the most increased case in accuracy was TIR, 5, and 7 in Case #8, which showed an improvement of about 11.4% in overall accuracy. This means that TIR was more contributory

Table 3. Accuracy assessment of MLC with multi-band + TIR band

(Unit: %)

Case	NO.	Band combination	Producer's accuracy (%)						User's accuracy (%)						Overall accuracy (%)
			Forest	Water	Crop	Grass	Dry stream	Urban	Forest	Water	Crop	Grass	Dry stream	Urban	
#1	1	4/5/6	94	92	49	85	85	59	87	88	64	70	41	72	76.2
	2	Thermal/4/5/6	95	92	51	90	82	64	88	88	75	72	39	76	**78.8**
	3	Thermal/4/5	96	91	51	90	79	72	91	88	73	74	38	80	**80.7**
	4	Thermal/4/6	89	43	46	35	70	32	78	44	48	26	19	68	**56.4**
	5	Thermal/5/6	94	91	52	80	85	67	90	89	68	73	37	76	**78.4**
#2	6	2/6/7	95	92	40	89	79	56	90	88	44	56	48	76	74.1
	7	Thermal/2/6/7	93	91	51	82	82	64	90	87	55	62	50	78	**77.1**
	8	Thermal/2/6	93	84	44	63	91	45	89	61	63	49	27	75	**68.7**
	9	Thermal/2/7	93	91	51	81	76	66	90	86	55	62	57	78	**77.5**
	10	Thermal/6/7	95	91	56	83	82	22	86	88	42	38	60	68	**66.6**
#3	11	4/6/7	95	91	58	86	85	27	87	84	43	54	64	68	69.7
	12	Thermal/4/6/7	95	91	57	85	82	41	87	86	52	58	57	69	**73.2**
	13	Thermal/4/6	89	43	46	35	70	32	78	44	48	26	19	68	**56.4**
	14	Thermal/4/7	95	91	56	85	76	44	90	88	44	56	63	73	**73.0**
	15	Thermal/6/7	95	91	56	83	82	22	86	88	42	38	60	68	**66.6**
#4	16	2/3/7	94	91	53	85	82	77	89	87	71	68	61	81	81.5
	17	Thermal/2/3/7	94	91	54	86	79	79	90	88	72	74	68	79	**82.4**
	18	Thermal/2/3	92	86	38	78	85	59	91	60	72	65	28	76	**72.6**
	19	Thermal/2/7	93	91	51	81	76	66	90	86	55	62	57	78	**77.5**
	20	Thermal/3/7	95	91	58	77	82	41	87	87	52	43	64	73	**71.9**
#5	21	3/5/7	95	92	52	88	79	81	91	88	77	81	57	79	83.2
	22	Thermal/3/5/7	95	91	55	86	79	82	91	88	81	81	60	79	**84.0**
	23	Thermal/3/5	95	93	54	88	85	72	91	89	73	77	42	80	**81.2**
#6	24	Thermal/5/7	94	92	52	85	79	80	91	88	75	78	55	78	**82.5**
	25	Thermal/3/7	95	91	58	77	82	41	87	87	52	43	64	73	**71.9**
	26	4/5/7	95	92	51	86	76	71	88	86	76	80	53	73	80.0
	27	Thermal/4/5/7	95	92	55	89	73	72	87	86	79	81	52	76	**81.2**
	28	Thermal/4/5	96	91	51	90	79	72	91	88	73	74	38	80	**80.7**
	29	Thermal/4/7	95	91	56	85	76	44	90	88	44	56	63	73	**73.0**
	30	Thermal/5/7	94	92	52	85	79	80	91	88	75	78	55	78	**82.5**
#7	31	2/5/7	93	93	51	84	76	79	91	87	75	64	51	81	81.6
	32	T/2/5/7	94	92	55	83	79	82	90	88	77	74	59	81	**83.0**
	33	Thermal/2/5	94	92	51	85	79	78	91	87	77	78	42	79	**81.7**
	34	Thermal/2/7	93	91	51	81	76	66	90	86	55	62	57	78	**77.5**
	35	Thermal/5/7	94	92	52	85	79	80	91	88	75	78	55	78	**82.5**
#8	36	5/6/7	91	96	21	84	52	64	87	84	48	52	23	73	71.1
	37	Thermal/5/6/7	95	92	51	85	73	70	88	85	75	79	46	74	**79.5**
	38	Thermal/5/6	94	91	52	80	85	67	90	89	68	73	37	76	**78.4**
	39	Thermal/5/7	94	92	52	85	79	80	91	88	75	78	55	78	**82.5**
	40	Thermal/6/7	95	91	56	83	82	22	86	88	42	38	60	68	**66.6**
#9	41	2/5/6	93	93	40	85	82	59	88	88	69	58	32	74	74.4
	42	Thermal/2/5/6	95	92	52	84	85	73	91	88	75	78	37	79	**80.6**
	43	Thermal/2/5	94	92	51	85	79	78	91	87	77	78	42	79	**81.7**
	44	Thermal/2/6	93	84	44	63	91	45	89	61	63	49	27	75	**68.7**
	45	Thermal/5/6	94	91	52	80	85	67	90	89	68	73	37	76	**78.4**
#10	46	3/6/7	95	92	48	80	85	29	86	87	50	34	55	66	67.3
	47	Thermal/3/6/7	95	91	58	77	85	40	87	87	52	44	57	73	**71.8**
	48	Thermal/3/6	93	19	43	56	85	30	73	26	50	40	22	73	**56.1**
	49	Thermal/3/7	95	91	58	77	82	41	87	87	52	43	64	73	**71.9**
	50	Thermal/6/7	95	91	56	83	82	22	86	88	42	38	60	68	**66.6**

to the accuracy improvement than Band 2 in Case #8 when classifying the land cover. In Case #4, overall accuracy improved by 1.2% in the cases of TIR, 2, 3, and 7 band combinations, but 3 band combinations that included TIR were decreased by an average of 7.5% in overall accuracy.

In three TIR band–included combinations, overall accuracy declined by 7.5% on average, which means that because the band that can identify near-infrared spectral characteristics was excluded, even though a TIR band was included, there was no improvement in overall accuracy.

Table 4. Average overall accuracy improvement in each case

(Unit: %)

Case	#1	#2	#3	#4	#5	#6	#7	#8	#9	#10
Overall accuracy improvement	4.5	3.4	3.5	0.9	0.8	2.5	1.4	11.4	7.4	4.6

In this study, when a TIR band was added to each case, the average overall accuracy improved in all cases, as summarized in Table 4. Therefore, overall accuracy improved in the band combinations in which a TIR band was added to a multi-band, compared to the band combinations without TIR bands. The improvement of overall accuracy by classification category is stated in Table 5.

In terms of the accuracy improvement in an urban area, in particular, producer's accuracy and user's accuracy were high: 10.2% and 3.8%, respectively. However, in water, producer's accuracy and user's accuracy were lowest: -0.7% and 1.7%, respectively. In water, a TIR band revealed little effect on the accuracy improvement.

As mentioned above, general multi-image bands are better than the combination of multiband images with TIR band added in terms of effects on classification accuracy at landuse/landcover classification in an urban area using Landsat 8 images.

Table 5. Comparison of improved accuracies by classes (average)

(Unit: %)

	Forest	Water	Crop	Grass	Dry Stream	Urban Area
P.A.	1.1	-0.7	9.5	0.8	6.6	10.2
U.A.	2.0	1.7	8.6	9.2	9.7	3.8

4. Conclusion

In this study, the practical usability of TIR band images was tested against Seoul and nearby areas with diverse land covers based on image classification, using Landsat 8 satellite images. In the test area, the combination of general multi images and TIR band images was greater than general multi-image bands by 4.0% in terms of classification accuracy. In an urban area, in particular, producer's accuracy and user's accuracy increased by 10.2% and 3.8%, respectively. Therefore, it appears that land cover classification and surface information analysis could be more accurate in an urban area where diverse land covers are found. With the addition of TIR bands to Landsat environmentally remote sensing satellite information, a study on the renewal of satellite image-based land cover classifications would therefore become more accurate.

Acknowledgement

This work is financially supported by Korea Ministry of Land, Infrastructure and Transport(MOLIT) as 「U-City Master and Doctor Course Grant Program」.

References

Chander, G. and Markham, B. (2003), Revised Landsat-5 TM radiometric calibration procedures and postcalibration dynamic ranges, *IEEE Transactions on Geoscience and Remote Sensing*, Vol. 41, No. 11, pp. 2674-2677.

Choi, J.W. (2011), *Hybrid Pansharpening Algorithm of High-Spatial Resolution Satellite Images by Extracting Automatic Parameter Based on Spatial Correlation*, Ph.D. dissertation, Graduate School of Seoul National University, Seoul, Korea, 114p. (in Korean with English abstract)

Choi, J.W. and Kim, Y.I. (2010), Pan-sharpening algorithm of high-spatial resolution satellite image by using spectral and spatial characteristics, *Journal of the Korean Society for Geospatial Information System*, Vol. 2, No. 18, pp. 79-86. (in Korean with English abstract)

Coll, C., Galve, J.M., Sanchez, J.M., and Caselles, V. (2010), Validation of Landsat-7/ETM+ TIR-band calibration and atmospheric correction with ground-based measurements, *IEEE Transactions on Geoscience and Remote Sensing*, Vol. 1, No. 48, pp. 547-555.

Eo, Y.D. (1999), *Development of the Training Normalization Algorithm and the Class Separability Measurement for Satellite Image Classification*, Ph.D. dissertation, Graduate School of Seoul National University, Seoul, Korea, 113p. (in Korean with English abstract)

Erdenechimeg, M., Choi, B.G., Na, Y.W., and Kim, T.H. (2010), Detection of land cover change using Landsat image data in desert area, *Journal of the Korean Society of Surveying, Geodesy, Photogrammetry and Cartography*, Vol. 2, pp. 471-476.

FLAASH (2009), *Atmospheric Correction Module: QUAC and FLAASH User's Guide*, Version 4. 7, ITT Visual Information Solutions Inc., Boulder, Co.

Jeganathan, C., Hamm, N.A.S., Mukherjee, S., Atkinson, P.M., Raju, P.L.N., and Dadhwal, V.K. (2011), Evaluating a TIR image sharpening model over a mixed agricultural landscape in India, *International Journal of Applied Earth Observation and Geoinformation*, Vol. 13, No. 2, pp. 178-191.

Jensen, J.R. (2007), *Remote Sensing of the Environment: An Earth Resource Perspective 2nd Edition*, Prentice Hall Series in Geographic Information Science, Pearson Prentice Hal Inc, New Jersey.

Jung, H.S. and Park, S.W. (2014), Multi-sensor fusion of Landsat 8 TIR and panchromatic images, *Sensors*, Vol. 14, No. 2, pp. 24425-24440.

Kim, Y.H. (2008), *Modified Substitute Wavelet Image Fusion Method-Application to IKONOS Image-*, Master's thesis, Graduate School of Seoul National University, Seoul, Korea, 46p. (in Korean with English abstract)

Kwon, B.K., Yamada, K., Niren, T., and Jo, M.H. (2003), A study on the landcover classification using band ratioing data of Landsat TM, *Journal of the Korean Association of Geographic Information Studies*, Vol. 2, No. 6, pp. 80-91. (in Korean with English abstract)

Lee, H.J., Kim, S.W., Brioude, J., Cooper, O.R., Frost, G.J., Kim, C.H., Park, R.J., Trainer, M., and Woo, J.H. (2014), Transport of NOx in East Asia identified by satellite and in situ measurements and lagrangian particle dispersion model simulations, *Journal of Geophysical Research: Atmospheres*, Vol. 119, No. 5, pp. 2574-2596.

Lee, S.B., La, P.H., Eo, Y.D., and Pyeon, M.W. (2015), Generation of simulated image from atmospheric corrected Landsat TM images, *Journal of the Korean Society of Surveying, Geodesy, Photogrammetry and Cartography*, Vol. 33, No. 1, pp. 1-9. (in Korean with English abstract)

Lee, H.S., Oh, K.Y., and Jung, H.S. (2014), Comparative analysis of image fusion methods according to spectral responses of high-resolution optical sensors, *Korean Journal of Remote Sensing*, Vol. 30, No. 2, pp. 227-239. (in Korean with English abstract)

Moon, C.Y., Lee, J.C., and Koo, J.H. (2012), *U-city Policy Handbook: A Guide to the Ubiquitous City Policy of Korea*, Sigma Press, Korea.

Park, M.E., Song, C.H., Park, R.S., Lee, J., Kim, J., Lee, S., Woo, J.-H., Carmichael, G.R., Eck, T.F., Holben, B.N., Lee, S.-S., Song, C.K., and Hong, Y.D. (2014), New approach to monitor transboundary particulate pollution over Northeast Asia, *Atmospheric Chemistry and Physics*, Vol. 14, No. 2, pp. 659-674.

Schneider, K. and Mauser, W. (1996), Processing and accuracy of Landsat thematic mapper data for lake surface temperature measurement, *International Journal of Remote Sensing*, Vol. 17, No. 11, pp. 2027-2041.

Sugumaran, R., Pavuluri, M.K., and Zerr, D. (2003), The use of high-resolution imagery for identification of urban climax forest species using traditional and rule-based classification approach, *IEEE Transactions on Geoscience and Remote Sensing*, Vol. 41, No. 9, pp. 1933-1939.

Warner, T.A. and Nerry, F. (2009), Does single broadband or multispectral TIR data add information for classification of visible, near-and shortwave infrared imagery of urban areas?, *International Journal of Remote Sensing*, Vol. 30, No. 9, pp. 2155-2171.

Zhang, J., Wang, Y., and Li, Y. (2006), A C++ program for retrieving land surface temperature from the data of Landsat TM/ETM+ band6, *Computers & Geosciences*, Vol. 32, No. 10, pp. 1796-1805.